Tuning stiffness of free-standing hydrogen-bonded LbL films with Fe^{3+} coordination

*Yu Yan, Matthew Feeney, Luke M. Davis, and Samuel W. Thomas III**

Department of Chemistry, Tufts University, 62 Talbot Avenue, Medford, MA 02155

ABSTRACT: Layer-by-layer (LbL) assembly of polymers through hydrogen bonding is a versatile technique for building ultra-thin functional films. However, the hygroscopic nature of the polymer building blocks and hydrogen bonding propensity of water can render the assembled films sensitive to environmental conditions, especially humidity, resulting in the low stiffness of such films. In this paper, we report a simple approach to crosslink free-standing hydrogen-bonded LbL films by coordination with iron(III). The stiffnesses of these films increased by three orders of magnitude upon crosslinking with Fe^{3+}, allowing the films to be handled and manipulated easily at high humidity. Moreover, we used the photo-induced reduction of the coordinated iron(III) ions to demonstrate the potential for tuning the mechanical properties of these films using light. In sum, this paper demonstrates a simple and effective approach for strengthening and tuning mechanical properties of hydrogen-bonded LbL films.

Keywords: Layer-by-layer, iron crosslinking, hydrogen bond, photochemistry, free-standing films

Introduction

Layer-by-layer (LbL) assembly is a versatile technique for depositing thin films with two or more components.[1–4] The extensive substrate compatibility of LbL includes macroscopic planar substrates such as silicon wafers or glass slides, microparticles and nanoparticles, cells, and a variety of other possibilities.[5] Moreover, LbL is applicable to a wide diversity of materials that can comprise the deposited thin film, including biopolymers such as DNA and proteins.[6] LbL also allows control over the thickness of either free-standing thin films or coatings on the nanoscale. Chemical modification of simple, commercial materials can further enhance these advantages of LbL assembly to yield functional materials for applications that include stimuli-responsive materials,[7,8] self-healing,[9,10] biocompatibility,[11] and drug delivery.[12]

The chemical design of such materials usually involves designing structural elements of polymers or other materials that participate in specific interactions between alternately deposited layers.[1] Although the most frequently used LbL systems rely on ion pairing between oppositely charged polyelectrolytes, other interactions such as hydrogen bonding are also broadly utilized.[13–15] Compared to ion-pairing analogs, hydrogen bonding LbL assemblies offer several advantages. For example, hydrogen bonding expands the library of polymeric building blocks beyond polyelectrolytes, which enables materials with increasingly tunable mechanical, physicochemical, optical, and even stimuli-responsive properties.[15] Also, such films can be disassembled on demand under mild conditions.[14,16] Moreover, because these films have only weak interactions with hydrophobic substrates, such LbL assemblies can be separated from their substrates to afford free-standing films.[17]

The layer-by-layer films described in this paper comprise structurally simple, commercially available polymers—poly(ethylene oxide) (PEO) and poly(acrylic acid) (PAA). Each of these polymers is biocompatible, water-soluble, and inexpensive. Combinations of these two polymers can form stable complexes through hydrogen bonding that have found use in drug delivery,[18] energy storage,[19] and shape-memory materials.[20] Moreover, PEO substituents are frequently used as solubilizing functional groups for otherwise insoluble materials.[21] The Sukhishvili group reported free-standing hydrogen bonding LbL films comprising PAA and PEO, held together with hydrogen bonding.[14,22] More recently, PAA/PEO free-standing films have been identified as candidates for applied functional materials. For instance, Sun's group studied the water-triggered self-healing and erasing of PAA/PEO films,[9] while Lutkenhaus and coworkers successively reported their tunable ion-transporting capability,[23] wetting behaviors,[24], and thermal properties.[25] Grunlan's group reported the gas permeability tuned by pH of similar PAA/PEO multi-layer films.[26]

Similar to many other polymeric materials,[27,28] PAA/PEO LbL films are highly sensitive to environmental conditions, especially including elevated humidity, which can cause such materials to become too soft to handle. Water molecules can hydrogen bond with polymers and reduce the physical crosslinking between polymer chains. For instance, the Hammond group reported that Young's modulus of PAA/PEO films changed by ~1,000× with variations in humidity.[17] Thus, applications of hydrogen bonding LbL films that may require variations in humidity would benefit from increased structural rigidity and resistance to degradation in response to water. This is especially true for free-standing films, which cannot rely on substrates for support. Various approaches to crosslinking hydrogen-bonding LbL films have appeared in the literature, including chemical,[29] thermal,[17] photochemical,[30] and ionic crosslinking.[31]

The general approach of coordinating carboxylic acid groups and iron(III) has been reported in the field of hydrogels.[32] For example, Zheng and coworkers developed a mechanically strong hydrogel by crosslinking poly(acrylamide-co-acrylic acid) with Fe^{3+}, and also concluded that Fe^{3+} crosslinks PAA through tricarboxyl complexes at pH 4, while more acidic or basic pH environments partially destroy these complexes.[33] Li, Zhao, and coworkers reported programmable 3D shape transformation of PAA/PEO blends by patterned crosslinking via ferric ion solution.[34] Moreover, because of the different coordination affinities between Fe^{2+} and Fe^{3+}, the mechanical properties of iron(III) crosslinked hydrogels can be tuned by redox chemistry triggered via electrochemistry[35,36] and photo-reduction.[37–39] However, to our knowledge, crosslinking with iron(III) has yet to be reported with H-bonded LbL systems. The limited thicknesses and mechanical strengths of many LbL films makes robust and tunable crosslinking strategies for this class of materials especially important. Therefore, this paper reports crosslinking PAA/PEO films through exposure to aqueous iron(III), which enhances their mechanical properties as free-standing thin films and enables their handling in high humidity conditions.

Experimental Section

Materials

Poly(acrylic acid) (M_W ca. 240,000, 25.8% solid in water) was purchased from Scientific Polymer Products. Poly(ethylene oxide) (M_W ca. 600,000) was purchased from Polysciences. Ferric chloride hexahydrate was purchased from Fischer Scientific. All materials were used without any further purification. Deionized (DI) water was used for all film fabrication and crosslinking.

Fabrication of PAA/PEO Films

PAA solutions and PEO solutions at concentrations of 0.2% (w/v) were prepared by dissolving the polymers separately in DI water followed by stirring overnight at ambient temperature. Then, the pH of the two solutions was adjusted to 2.5 with 1 M HCl and 1 M NaOH aqueous solutions. An acidic rinsing solution was also prepared by adding 1 M HCl into DI water until the pH reached 2.5. The solutions were then filtered to remove any insoluble residues. Each filtrate was transferred into separate containers of a Midas III Automated Slide Stainer, which enables simultaneous immersion of up to 20 substrates following a user-programmed sequence. Polypropylene (PP) sheets (1/16-inch thickness, McMaster-Carr) were used as substrates for film deposition. PP substrates were cut into ~7.5 cm × 2.5 cm rectangles and washed by sequential sonication in ethanol and DI water. The slide stainer was programmed to first immerse the substrate in the PEO solution for 5 minutes, followed by two rinsing steps (one of 4 minutes and a second of 1 minute) in separate pH 2.5 rinsing solutions. These substrates were then immersed into the PAA solution, rinsed for 5 minutes as described above, to then yield a polymer bilayer deposited on each PP substrate. After approximately 20 hours, 60-bilayer coatings were obtained. All films were air-dried overnight in the ambient environment.

Crosslinking of PAA/PEO Films with Fe^{3+}

Air-dried PAA/PEO films on PP substrates were immersed into an aqueous solution of ferric chloride for 10 minutes. Different concentrations of Fe^{3+} afforded films with different degrees of crosslinking. The films were then rinsed by immersion in a pH 2.5 rinsing solution for 10 minutes to remove weakly bound iron ions. After air-drying overnight, the crosslinked films could be peeled off their PP substrates with tweezers to afford free-standing films.

Film Characterization.

Characterization experiments were performed at least three times unless described otherwise. To avoid the effect of material aging, the mechanical properties of all films were tested within three days of their preparation. The absorbances of free-standing films were measured by a UV/vis spectrophotometer in double-beam mode using a quartz glass for background subtraction spectra. The free-standing films analyzed by spectrophotometry were placed onto a quartz glass substrate before acquiring spectra.

Attenuated Total Reflection Fourier transform infrared (ATR-FTIR) spectroscopy was performed using a Jasco FTIR 6200 spectrometer equipped with PIKE Technologies Single Reflection MIRacle ATR accessory. Baseline-corrected spectra were collected in transmittance mode over a range of 600–4000 cm^{-1} at 4 cm^{-1} resolution and averaged over 32 scans to improve the signal-to-noise ratio. All the FT-IR tests were directly performed on the free-standing films over an area of ca. 1 cm^2 under ambient conditions.

Tensile testing of thin films was performed on a TA Instruments RSA3 Dynamic Mechanical Analyzer (TA Instruments, New Castle, DE). Measurements were performed under ambient conditions, with relative humidity measured and noted. Prepared films were cut into rectangular shapes, typically 10 mm × 15 mm. All samples (except those that were photoirradiated) were equilibrated in the dark for at least 30 minutes before testing. Strain-controlled measurements were performed in transient mode, at a constant strain rate of 0.1 mm per second.

Differential scanning calorimetry was performed with a TA Discovery 250 DSC under constant nitrogen flow. Heat-cool-heat cycles were performed on the films with ramp rates for both heating and cooling of 10 ºC/min. The data were collected from the second heating process to avoid artifacts from the thermal history of samples.

Microscopy

Field-emission scanning electron microscopy (FE-SEM) was performed with an AMRAY 1845 FE-SEM with SEMView8000, refurbished by SEMTech Solutions (North Billerica, MA). Sample coupons ca. 0.5-2 cm^2 were cut for SEM imaging with scissors. Cross-sections were obtained by gently scoring the film near one edge with a razor blade and peeling back the film. Samples were then mounted on aluminum stubs using carbon adhesives. Samples were coated with 5-10 nm of sputtered gold, to limit charging during imaging, using a Polaron SC502 sputter coater.

Energy-dispersive X-ray spectroscopy (EDS) was performed using the SEM beam and a Thermo Scientific Noran System 6 detector. The EDS detector is mounted normal to the imaging beam, so the sample stage was tilted 20° towards the detector during analysis. All samples were analyzed at 2000× magnification, 15 kV imaging voltage, and a working distance of 22 mm. Preliminary experiments showed that the number of iron counts observed at a single location was sensitive to the working distance, and maximized around 22 mm. EDS maps were collected from at least four locations on all iron-containing films and averaged. For the uncrosslinked film, two locations were sampled and both showed no iron (0 counts in both locations).

Photo-responsiveness

Each film was irradiated with a 200 W Hg/Xe lamp equipped with a condensing lens, water filter, and manual shutter. Wavelengths of irradiation were selected with appropriate filters. The power density varied between 30-70 mW/cm^2 when different filters were applied. Alternatively, films were irradiated with a hand-held UV lamp (235/365 nm, 2 mW/cm^2). To measure the variation in stiffness, films were left on the PP substrates for irradiation and equilibration until subjected to tensile testing. A set of films were irradiated with the same light source a day before the tensile test and stored in the dark, which allows all the tensile tests to be performed on the same

day, to minimize the impact of environmental conditions. Reversibility tests were carried out by peeling crosslinked films off the PP substrate and placing them on a piece of quartz glass, and then subjecting them to cycles of irradiating and storing in the dark. Changes in absorbance due to iron photoreduction, and subsequent air oxidation, were monitored by UV-vis spectrophotometry.

Results and Discussion

PAA/PEO films were assembled with a method adapted from Hammond and coworkers, which is driven by a combination of hydrophobic interactions and hydrogen bonding.[17] Films were produced by a simple procedure of immersing rectangular pieces of polypropylene sheet alternately in aqueous solutions of PEO and PAA (0.2% w/v), with intermediate rinsing steps to remove weakly adsorbed polymer (Figure 1). The polymer and rinsing solutions were held at pH 2.5 to maintain a high degree of protonation of PAA necessary for hydrogen bonding.[40] Peeling the film off the polypropylene substrates was routinely successful when the relative humidity (RH) was lower than 25%, yielding elastic free-standing films. These films are transparent to visible wavelengths of light and showed no obvious defects or pinholes under scanning electron microscopy (SEM), as shown in the supporting information. The thickness of these 60-bilayer films, as determined by SEM imagine of their cross-sections, was 3-5 μm which is comparable with previously reported PAA/PEO films.[23,25]. Differential scanning calorimetry (DSC) revealed only one glass transition temperature (T_g) at 65 °C, indicating the polymers are fully miscible with each other, without crystalline PEO in the films.[17]

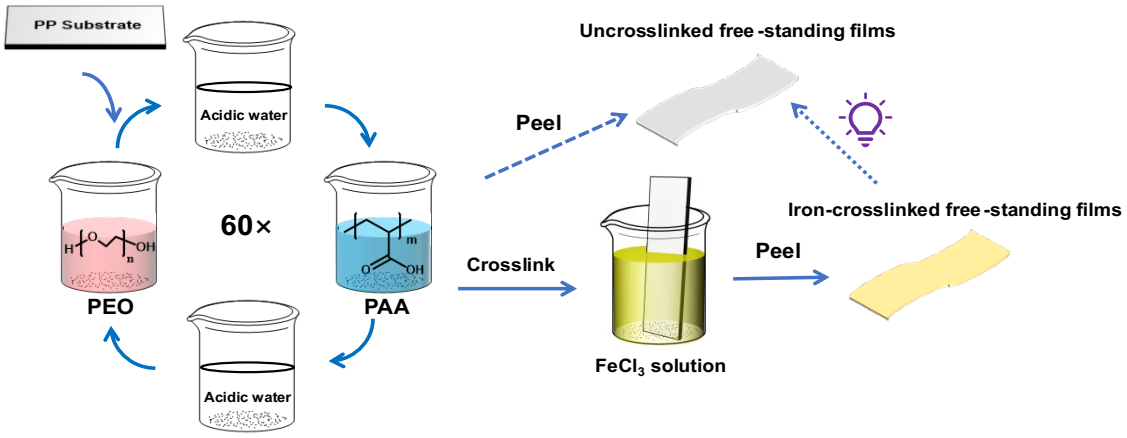

Figure 1: Fabrication of iron-crosslinked free-standing films.

The mechanical properties of these PAA/PEO films depend strongly on the environmental humidity, in that they lose mechanical integrity at higher humidity. In contrast to the easily handled films prepared at low RH, films prepared at RH higher than 40% were soft and easily deformable, making it difficult to peel them from the substrate. At even higher relative humidity (RH > 60%), the films resembled gelatinous, viscous liquids that fail to hold their own shape. To investigate this phenomenon quantitatively, we performed tensile testing on the free-standing films. The calculated Young's Moduli of these films varied from approximately 1 kPa (RH > 40%) to approximately 200 kPa (RH < 25%). We note that the range of Young's Moduli for similar films is known to be even broader: under more rigorously dried conditions the Young's Modulus of PAA/PEO free-standing films has been reported to be as high as 6.7 MPa.[17] Therefore, although these films maintain mechanical integrity at low humidity, water swells the polymer network at higher humidity levels, rendering these materials unusably soft as free-standing films by interrupting interchain hydrogen bonding.

Given the deleterious impact of humidity on these films, we expected that presence of a secondary crosslinker could maintain the mechanical properties of such films at higher humidity.

Kharlampieva and coworkers have reported improving the mechanical robustness with hydrogen-bonded thin films with Zr(IV) crosslinking that could be reversed by exposure to EDTA.[41] The enhanced ultrathin polymeric films with thicknesses less than 100 nm were able to keep its shape after releasing from the substrates and yielded "free-floating" hydrogels, but required etching of a SiO2 sacrificial layer. Crosslinking gels by simply soaking in a multivalent ion solution is a simple, effective, and low-cost method for improving film stability,[32] and is well established for hydrogels such as those made from the polysaccharide alginate.[42] We therefore tested the impact of seven multivalent ions by immersing the films into 5 mM solutions for 10 minutes followed by 10-minute rinsing with pH 2.5 solutions. Among these metal cations investigated, iron(III) provided a significant enhancement of Young's moduli (~100×) while the others—including aluminum(III) and iron(II)—did so by less than one order of magnitude (Figure S10). Therefore, in the remainder of this work, we focused on iron(III) as a crosslinker. The coordination between iron(III) and ligands on the polymer chains (likely carboxylic acid groups) was achieved by simply immersing films in an aqueous solution of $FeCl_3$ at concentrations of 1-20 mM for 10 minutes, followed by washing the films with pH 2.5 water. After drying under ambient conditions overnight, the films were a pale-yellow color, which could be recognized by eye and quantitively measured with UV-vis spectroscopy, indicating the incorporation of iron(III) ions (Figure S15).

Analysis by SEM did not reveal any noticeable changes in the morphology of the films after crosslinking. Caruso and coworkers reported a similar observation in their report on multivalent ion crosslinking of other hydrogen-bonding LbL films with iron(III).[31] The thickness of the films was not significantly impacted by exposure to iron solutions according to our observation under SEM. After exposure to iron(III) solutions, we could readily peel all films off the polypropylene substrates, even when RH > 40%. The glass transition temperatures of the free-standing films

determined by DSC (66 °C) were unchanged from before crosslinking. This observation both demonstrates the enhancement of the mechanical properties of the films through crosslinking and addresses the practical problem of forming free-standing films of hydrogen bonding LbL films at higher levels of humidity.

To better understand and optimize the crosslinking process, we varied the Fe^{3+} immersion times and concentrations. As Figure 2 shows, the cross-linking of these films with iron increased the absorbance significantly in the range of 200-450 nm, consistent with previous observations during the crosslinking of alginate gels[34] and PAA/PEO complexes.[35] Importantly, absorbance at wavelengths longer than 250 nm is due only to the presence of iron(III) complexes, as confirmed by comparing the spectrum shape of free Fe^{3+} solution and Fe^{3+}-PAA complex solution (Figure S12). Moreover, the absorbance value of such solutions correlate with the concentration of Fe^{3+} ions when excess PAA was used (Figure S13). Therefore, we could estimate the relative amount of iron(III) incorporated in these films by their absorbance values at 365 nm (Figure S13 and Table S1). We varied the immersion time by dipping PAA/PEO films in 1 mM $FeCl_3$ solutions between 1 to 30 minutes . As expected, films immersed in Fe^{3+} solutions for longer times showed larger absorbance values than those immersed for shorter times, increasing from 0.06 to about 0.23. With immersions longer than 20 minutes, however, the shape of the absorbance spectrum changed, and the films cracked after drying (Figure S1). To avoid this over-exposure, we selected 10 minutes for all subsequent experiments.

With this crosslinking process, the absorbances of the films at 365 nm correlate positively with the concentration of Fe^{3+} in the immersion solutions, revealing the possibility of precise control over the extent of crosslinking through concentration. Moreover, EDS experiments are consistent with the trend we interpreted from the absorbance. Both iron and chlorine counts increased with

the absorbance of the films, supporting the relationship between the absorbance and the amount of iron incorporated within the polymer films (Figure S5, S6). Finally, we estimate a 5 μm-thick film PAA/PEO film has on the order of 1 mmol of carboxylic acid groups in the entire film, which is more than the entirety of Fe^{3+} ions in the crosslinking solutions for even the highest concentration that we tested (30 mL of 15 mM Fe^{3+}), indicating that only a small fraction of available carboxylates in the films ligate to iron ions upon exposure to the Fe^{3+} solution.

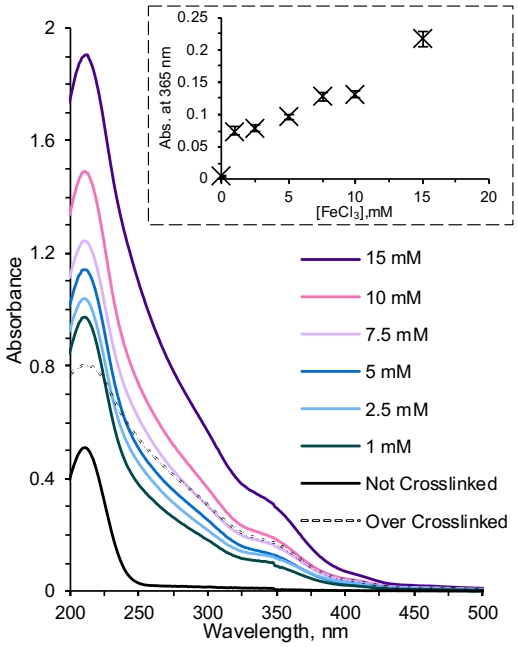

Figure 2. The absorbance of iron-crosslinked films. Inset: the dependence of the absorbance of the films at 365 nm on the concentrations of $FeCl_3$ solutions.

The work of Zheng and coworkers supports the complexation of carboxylate functional groups of with Fe^{3+} in PAA-based hydrogels.[33] In our crosslinked LbL films reported here, we observed only modest changes in the shapes of FT-IR spectra of these films with increasing Fe^{3+} incorporation, suggesting that even at the highest concentration of Fe^{3+}, the vast majority of

carboxylate functional groups remain uncrosslinked. Both our estimate of the sub-stoichiometric amount of available Fe^{3+} ions in the entirety of the crosslinking solution (*vide supra*), and the acidic pH (2.5) ensuring that >90% of carboxylate functional groups are protonated further support this conclusion. As shown in Figure S16, all the samples displayed characteristic peaks at 1700-1750 cm^{-1} and 1050-1100 cm^{-1}, corresponding to the stretching of carbonyl group (C=O) in PAA and the vibration of ether bonds (C-O-C) in PEO, respectively.[20] Moreover, with the concentration of incorporated iron increasing, small peaks or shoulders appeared at 1590, 1160, 1030, and 790 cm^{-1}, suggesting changes in the bonding nature within the polymeric films due to incorporation of Fe^{3+} ions.[43–45] In particular, the small peak at 1590 cm^{-1} has been observed previously in Fe^{3+}-crosslinked PAA-chitosan nanofibers, and has been ascribed to bidentate bridging complexes.[46] A carboxylate-iron bond is also supported by Fe^{3+} perturbing the peak at 1160 cm^{-1}, which has been ascribed previously to C-O stretching coupled to the O-H bend in PAA.[47]

The free-standing nature of the films enabled characterization of their mechanical properties by standard tensile testing. The Young's Moduli of the films were calculated from the linear regime (strain < 5%) using thicknesses of 3.5 μm for all films, based on our SEM analysis. Given the sensitivity of these films to ambient humidity, we performed each set of tensile testing on films with varying levels of Fe^{3+} incorporation all on the same day, with films from the same batch of fabrication processes. To understand the influence of ambient humidity on the properties of these films, we also repeated this suite of experiments on films prepared using the same fabrication protocols on other days with different ambient relative humidity levels.

Figure 3 shows the stress-strain curves of films crosslinked with different amounts of Fe^{3+} at RH ~ 40%. In general, increasing the concentration of Fe^{3+} increased the stiffness and ultimate stress of crosslinked films, and decreased their strain at fracture. Young's moduli of these films were

calculated from the slope in the elastic regime of the curves. The modulus of these films increased from 1-2 kPa for uncrosslinked films to 33 kPa for films treated with 1 mM $FeCl_3$ solution, and further to 0.20 MPa when using 10 mM solution. However, the elongation at fracture decreased from 440% to only 50% with concentrations higher than 10 mM. Zheng and coworkers reported a similar trend in their study of how iron(III) crosslinks poly(acrylamide-co-acrylic acid) hydrogels by coordination.[36]

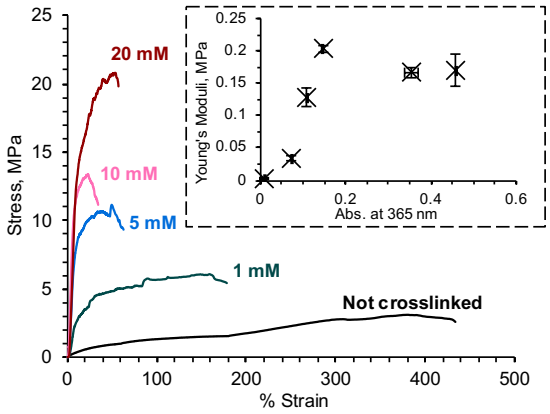

Figure 3. Tensile testing curves of free-standing films exposed to varying concentrations of Fe^{3+} crosslinker. The experiment was performed at RH ~ 40%. Inset: Calculated Young's moduli as a function of absorbance of films at 365 nm. The error bars represent the double standard error of the mean calculated from at least 3 successive tests on different films under the same conditions.

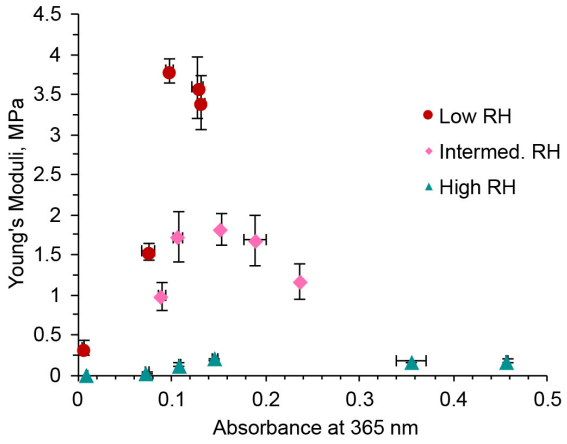

Figure 4. Dependence of Young's Moduli of free-standing LbL films on relative humidity and their absorbance at 365 nm, achieved by immersing films in different concentrations of Fe^{3+} for 10 minutes. The tensile tests were performed 3 times under high relative humidity (RH ~ 40%, triangle, green), intermediate relative humidity (RH ~ 30%, diamond, pink), and low relative humidity (RH < 25%, round, brown). The error bars represent the standard error of the mean calculated from at least three successive tests under the same conditions.

We further probed the impact of moisture on the mechanical properties of crosslinked films, particularly stiffness, with additional sets of tensile tests performed under different relative humidities. The dependence of calculated Young's Moduli on both relative humidity and incorporation of Fe^{3+} is shown in Figure 4. While increasing the density of crosslinking did stiffen these films regardless of humidity, these films also maintained sensitivity towards humidity after crosslinking, indicating the importance of hydrogen bonding in the structure of these films. As an example of these trends, the moduli of films with similar concentrations of Fe^{3+} (absorbance ~ 0.11) increased from 0.13 MPa at high RH (> 40%) to 1.7 MPa at intermediate RH (~33%), and was as high as 3.8 MPa at low RH (< 25%). In addition, when using an iron(III) solution with a concentration higher than 20 mM, although the absorbance could still increase, the stiffness of the

films reached a plateau or even decreased slightly. The same trend has been observed by others in similar systems, who attribute this phenomenon to the decreased stability constant of the coordination resulting from the increasing acidity of the environment.[36–38]

Carboxylate-Fe^{3+} complexes are known to undergo reduction by chemical reductants[31] or light,[38] resulting in the formation of Fe^{2+} and sacrificial release of carbon dioxide.[50] With a lower oxidation state, Fe^{2+} crosslinks carboxylate-containing polymers less efficiently, in agreement with our observation that treatment of PAA/PEO LbL films with divalent metal ions does not substantially increase their stiffness. Therefore, irradiation of Fe^{3+} crosslinked materials can reduce their mechanical strength.[35,37,38] In this work, we used UV light to control the stiffness of the iron-crosslinked PAA/PEO LbL films. As shown in Figure 5, irradiating (20 minutes, 2 mW/cm^2) a film crosslinked with 5 mM Fe^{3+} decreased in stiffness by 30% (0.64 MPa to 0.45 MPa). Meanwhile, the absorbance at 365 nm decreased by 17% due to the reduction of Fe^{3+} to Fe^{2+}, which has reduced extinction efficiency in the UV.[38] The iron in these films could be re-oxidized by storing the film in the dark under otherwise ambient conditions.[38] The stiffness recovered past the original value by approximately 30%, and the strain at break fell from 15% to 8%. We suspect that rearrangements of the cross-linking occurred during the cycle of iron reduction and oxidation, in addition to chemical changes within the films due to the irreversible nature of the overall chemical reaction. The impact of irreversible changes was further evidenced by repeating the irradiation/oxidation cycle three times (see supporting information), in that there was some reversion of the absorbance with each step, but with noticeable fatigue. Furthermore, evidence for a cycle of photoreduction/air oxidation of the iron ions in these films arose from selective 1,10-phenanthroline complexation of Fe^{2+}. The signature absorbance peak of Fe^{2+}-*phen* complex (515 nm) appeared only after the film was irradiated.[51] Subsequently, the absorbance due to this

complex decreased when irradiated films were stored in the dark, consistent with re-oxidation to Fe^{3+} (Figure S14).

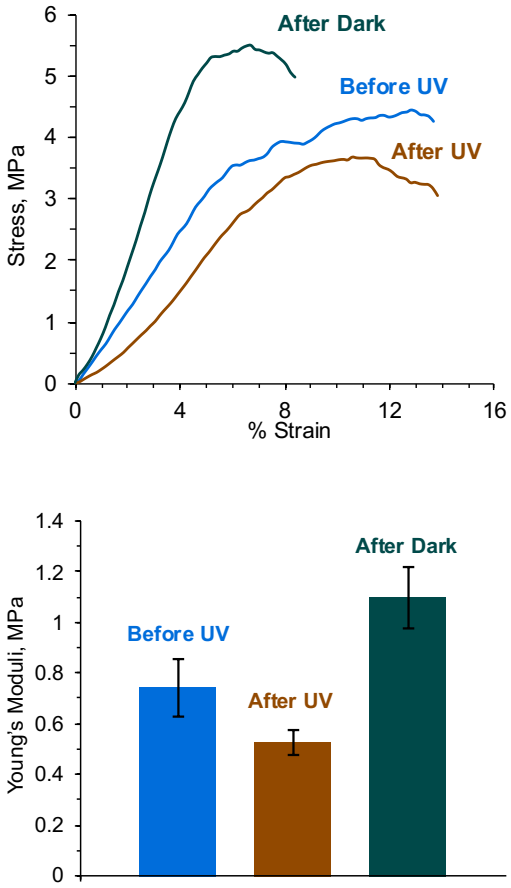

Figure 5. TOP: Tensile curves of films before irradiation (Before UV, pink), after UV irradiation for 20 minutes (After UV, brown), and after storing in the dark for a day after irradiation (After Dark, green). All the tests were performed on the same day using films from the same batch and the same crosslinking process. BOTTOM: The Young's Moduli of iron-crosslinked films without irradiation (Before UV, pink), irradiated for 20 minutes (After UV, brown), and kept in dark for one day after irradiation (After Dark, green). All the tests were performed on the same day using films from the same batch and the same crosslinking process. The error bars represent the standard errors of the means calculated from at least 3 successive tests.

Conclusion

We have developed an operationally simple method to overcome the poor mechanical stability of hydrogen-bonded PAA/PEO LbL films under high humidity environments. These films contain inexpensive polymers and readily can be assembled to a thickness of microns. The ionic crosslinking method is synthesis-free, low-cost, and readily controlled through ion concentration. The crosslinked films are also reversibly photo-responsive, which allows the use of light to modulate their mechanical properties. Disadvantages of this approach include low photo-reduction efficiency, a limitation to acidic environments, and challenges in quantitatively precise control of light-induced modulation. We anticipate that our work could provide alternative approaches for improving and tuning the mechanical stability and stiffness of various LbL films, which has the potential for impact in controlling cell adhesion or drug delivery.[39,40]

ASSOCIATED CONTENT

Supporting Information. SEM images and DSC traces of LbL films, impact of different metal ions on Young's Moduli of free-standing LbL films, and reversibility of photoreduction of Fe^{3+}-crosslinked films (PDF).

AUTHOR INFORMATION

Corresponding Author

*Email: sam.thomas@tufts.edu

ACKNOWLEDGMENT

This work was supported by the National Science Foundation (CHE-1806263). The authors thank Thomas Falcucci and Prof. David Kaplan for assistance with tensile testing.

REFERENCES

(1) Borges, J.; Mano, J. F. Molecular Interactions Driving the Layer-by-Layer Assembly of Multilayers. *Chem. Rev.* **2014**, *114* (18), 8883–8942. https://doi.org/10.1021/cr400531v.

(2) Li, Y.; Wang, X.; Sun, J. Layer-by-Layer Assembly for Rapid Fabrication of Thick Polymeric Films. *Chem. Soc. Rev.* **2012**, *41* (18), 5998–6009. https://doi.org/10.1039/c2cs35107b.

(3) Zhao, S.; Caruso, F.; Dahne, L.; Decher, G.; De Geest, B. G.; Fan, J.; Feliu, N.; Gogotsi, Y.; Hammond, P. T.; Hersam, M. C.; et al. The Future of Layer-by-Layer Assembly: A Tribute to ACS Nano Associate Editor Helmuth Mohwald. *ACS Nano* **2019**, *13* (6), 6151–6169. https://doi.org/10.1021/acsnano.9b03326.

(4) Decher, G.; Lehr, B.; Lowack, K.; Lvov, Y.; Schmitt, J. Layer-by-Layer Adsorbed Films of Polyelectrolytes, Proteins or DNA. *Biosens. Bioelectron.* **1994**, *9*, 677–684.

(5) Ariga, K.; Lvov, Y.; Decher, G. There Is Still Plenty of Room for Layer-by-Layer Assembly for Constructing Nanoarchitectonics-Based Materials and Devices. *Phys. Chem. Chem. Phys.* **2022**, *24* (7), 4097–4115. https://doi.org/10.1039/d1cp04669a.

(6) Saurer, E. M.; Flessner, R. M.; Sullivan, S. P.; Prausnitz, M. R.; Lynn, D. M. Layer-by-Layer Assembly of DNA- and Protein-Containing Films on Microneedles for Drug Delivery to the Skin. *Biomacromolecules* **2010**, *11* (11), 3136–3143. https://doi.org/10.1021/bm1009443.

(7) Hu, X.; McIntosh, E.; Simon, M. G.; Staii, C.; Thomas, S. W. Stimuli-Responsive Free-Standing Layer-By-Layer Films. *Adv. Mater.* **2016**, *28* (4), 715–721. https://doi.org/10.1002/adma.201504219.

(8) Feeney, M. J.; Thomas, S. W. Combining Top-Down and Bottom-Up with Photodegradable Layer-by-Layer Films. *Langmuir* **2019**. https://doi.org/10.1021/acs.langmuir.9b02005.

(9) Wang, Y.; Li, T.; Li, S.; Guo, R.; Sun, J. Healable and Optically Transparent Polymeric Films Capable of Being Erased on Demand. *ACS Appl. Mater. Interfaces* **2015**, *7* (24), 13597–13603. https://doi.org/10.1021/acsami.5b03179.

(10) Skorb, E. V.; Andreeva, D. V. Layer-by-Layer Approaches for Formation of Smart Self-Healing Materials. *Polym. Chem.* **2013**, *4* (18), 4834–4845. https://doi.org/10.1039/c3py00088e.

(11) Correa, S.; Boehnke, N.; Barberio, A. E.; Deiss-Yehiely, E.; Shi, A.; Oberlton, B.; Smith, S. G.; Zervantonakis, I.; Dreaden, E. C.; Hammond, P. T. Tuning Nanoparticle Interactions with Ovarian Cancer through Layer-by-Layer Modification of Surface Chemistry. *ACS Nano* **2020**, *14* (2), 2224–2237. https://doi.org/10.1021/acsnano.9b09213.

(12) Alkekhia, D.; Hammond, P. T.; Shukla, A. Layer-by-Layer Biomaterials for Drug Delivery. *Annu. Rev. Biomed. Eng.* **2020**, *22*, 1–24. https://doi.org/10.1146/annurev-bioeng-060418-052350.

(13) Cheung, J. H.; Stockton, W. B.; Rubner, M. F. Molecular-Level Processing of Conjugated Polymers. 3. Layer-by-Layer Manipulation of Polyaniline via Electrostatic Interactions. *Macromolecules* **1997**, *30* (9), 2712–2716. https://doi.org/10.1021/ma970047d.

(14) Sukhishvili, S. A.; Granick, S. Layered, Erasable Polymer Multilayers Formed by Hydrogen-Bonded Sequential Self-Assembly. *Macromolecules* **2002**, *35* (1), 301–310. https://doi.org/10.1021/ma011346c.

(15) Kharlampieva, E.; Koziovskaya, V.; Sukhishvili, S. A. Layer-by-Layer Hydrogen-Bonded Polymer Films: From Fundamentals to Applications. *Adv. Mater.* **2009**, *21* (30), 3053–3065. https://doi.org/10.1002/adma.200803653.

(16) Such, G. K.; Johnston, A. P. R.; Caruso, F. Engineered Hydrogen-Bonded Polymer Multilayers: From Assembly to Biomedical Applications. *Chem. Soc. Rev.* **2011**, *40* (1), 19–29. https://doi.org/10.1039/c0cs00001a.

(17) Lutkenhaus, J. L.; Hrabak, K. D.; McEnnis, K.; Hammond, P. T. Elastomeric Flexible Free-Standing Hydrogen-Bonded Nanoscale Assemblies. *J. Am. Chem. Soc.* **2005**, *127* (49), 17228–17234. https://doi.org/10.1021/ja053472s.

(18) Kim, B.; Park, S. W.; Hammond, P. T. Hydrogen-Bonding Layer-by-Layer-Assembled Biodegradable Polymeric Micelles as Drug Delivery Vehicles from Surfaces. *2* (2), 386–392.

(19) Wang, Z.; Ouyang, L.; Li, H.; Wågberg, L.; Hamedi, M. M. Layer-by-Layer Assembly of Strong Thin Films with High Lithium Ion Conductance for Batteries and Beyond. *Small* **2021**, *17* (32). https://doi.org/10.1002/smll.202100954.

(20) Zou, S.; Lv, R.; Tong, Z.; Na, B.; Fu, K.; Liu, H. In Situ Hydrogen-Bonding Complex Mediated Shape Memory Behavior of PAA/PEO Blends. *Polymer (Guildf)*. **2019**, *183* (September), 121878. https://doi.org/10.1016/j.polymer.2019.121878.

(21) Feeney, M. J.; Thomas, S. W. Tuning the Negative Photochromism of Water-Soluble Spiropyran Polymers. *Macromolecules* **2018**, *51* (20), 8027–8037. https://doi.org/10.1021/acs.macromol.8b01915.

(22) Sukhishvili, S. A.; Granick, S. Layered , Erasable , Ultrathin Polymer Films. **2000**, *1* (15), 9550–9551.

(23) Lutkenhaus, J. L.; McEnnis, K.; Hammond, P. T. Tuning the Glass Transition of and Ion Transport within Hydrogen-Bonded Layer-by-Layer Assemblies. *Macromolecules* **2007**, *40* (23), 8367–8373. https://doi.org/10.1021/ma0713557.

(24) Seo, J.; Lutkenhaus, J. L.; Kim, J.; Hammond, P. T.; Char, K. Effect of the Layer-by-Layer (LbL) Deposition Method on the Surface Morphology and Wetting Behavior of Hydrophobically Modified PEO and PAA LbL Films. *Langmuir* **2008**, *24* (15), 7995–8000. https://doi.org/10.1021/la800906x.

(25) Sung, C.; Vidyasagar, A.; Hearn, K.; Lutkenhaus, J. L. Effect of Thickness on the Thermal Properties of Hydrogen-Bonded LbL Assemblies. *Langmuir* **2012**, *28* (21), 8100–8109. https://doi.org/10.1021/la301300h.

(26) Xiang, F.; Ward, S. M.; Givens, T. M.; Grunlan, J. C. Structural Tailoring of Hydrogen-Bonded Poly(Acrylic Acid)/Poly(Ethylene Oxide) Multilayer Thin Films for Reduced Gas Permeability. *Soft Matter* **2015**, *11* (5), 1001–1007. https://doi.org/10.1039/c4sm02363c.

(27) Nolte, A. J.; Treat, N. D.; Cohen, R. E.; Rubner, M. F. Effect of Relative Humidity on the Young's Modulus of Polyelectrolyte Multilayer Films and Related Nonionic Polymers. *Macromolecules* **2008**, *41* (15), 5793–5798. https://doi.org/10.1021/ma800732j.

(28) Ishiyama, C.; Higo, Y. Effects of Humidity on Young's Modulus in Poly(Methyl Methacrylate). *J. Polym. Sci. Part B Polym. Phys.* **2002**, *40* (5), 460–465. https://doi.org/10.1002/polb.10107.

(29) Kozlovskaya, V.; Ok, S.; Sousa, A.; Libera, M.; Sukhishvili, S. A. Hydrogen-Bonded Polymer Capsules Formed by Layer-by-Layer Self-Assembly. *Macromolecules* **2003**, *36* (23), 8590–8592. https://doi.org/10.1021/ma035084l.

(30) Sung, Y. Y.; Rubner, M. F. Micropatterning of Polymer Thin Films with PH-Sensitive and Cross-Linkable Hydrogen-Bonded Polyelectrolyte Multilayers. *J. Am. Chem. Soc.* **2002**, *124* (10), 2100–2101. https://doi.org/10.1021/ja017681y.

(31) Quinn, J. F.; Caruso, F. Multivalent-Ion-Mediated Stabilization of Hydrogen-Bonded Multilayers. *Adv. Funct. Mater.* **2006**, *16* (9), 1179–1186. https://doi.org/10.1002/adfm.200500530.

(32) Li, H.; Yang, P.; Pageni, P.; Tang, C. Recent Advances in Metal-Containing Polymer Hydrogels. *Macromol. Rapid Commun.* **2017**, *38* (14), 1–9. https://doi.org/10.1002/marc.201700109.

(33) Zheng, S. Y.; Ding, H.; Qian, J.; Yin, J.; Wu, Z. L.; Song, Y.; Zheng, Q. Metal-Coordination Complexes Mediated Physical Hydrogels with High Toughness, Stick-Slip

Tearing Behavior, and Good Processability. *Macromolecules* **2016**, *49* (24), 9637–9646. https://doi.org/10.1021/acs.macromol.6b02150.

(34) Li, G.; Wang, S.; Liu, Z.; Liu, Z.; Xia, H.; Zhang, C.; Lu, X.; Jiang, J.; Zhao, Y. 2D-to-3D Shape Transformation of Room-Temperature-Programmable Shape-Memory Polymers through Selective Suppression of Strain Relaxation. *ACS Appl. Mater. Interfaces* **2018**, *10* (46), 40189–40197. https://doi.org/10.1021/acsami.8b16094.

(35) Calvo-Marzal, P.; Delaney, M. P.; Auletta, J. T.; Pan, T.; Perri, N. M.; Weiland, L. M.; Waldeck, D. H.; Clark, W. W.; Meyer, T. Y. Manipulating Mechanical Properties with Electricity: Electroplastic Elastomer Hydrogels. *ACS Macro Lett.* **2012**, *1* (1), 204–208. https://doi.org/10.1021/mz2001548.

(36) Auletta, J. T.; Ledonne, G. J.; Gronborg, K. C.; Ladd, C. D.; Liu, H.; Clark, W. W.; Meyer, T. Y. Stimuli-Responsive Iron-Cross-Linked Hydrogels That Undergo Redox-Driven Switching between Hard and Soft States. *Macromolecules* **2015**, *48* (6), 1736–1747. https://doi.org/10.1021/acs.macromol.5b00142.

(37) Giammanco, G. E.; Sosnofsky, C. T.; Ostrowski, A. D. Light-Responsive Iron(III)-Polysaccharide Coordination Hydrogels for Controlled Delivery. *ACS Appl. Mater. Interfaces* **2015**, *7* (5), 3068–3076. https://doi.org/10.1021/am506772x.

(38) Giammanco, G. E.; Carrion, B.; Coleman, R. M.; Ostrowski, A. D. Photoresponsive Polysaccharide-Based Hydrogels with Tunable Mechanical Properties for Cartilage Tissue Engineering. *ACS Appl. Mater. Interfaces* **2016**, *8* (23), 14423–14429. https://doi.org/10.1021/acsami.6b03834.

(39) Ju, M.; Wu, B.; Sun, S.; Wu, P. Redox-Active Iron-Citrate Complex Regulated Robust Coating-Free Hydrogel Microfiber Net with High Environmental Tolerance and Sensitivity. *Adv. Funct. Mater.* **2020**, *30* (14), 1–7. https://doi.org/10.1002/adfm.201910387.

(40) Swift, T.; Swanson, L.; Geoghegan, M.; Rimmer, S. The PH-Responsive Behaviour of Poly(Acrylic Acid) in Aqueous Solution Is Dependent on Molar Mass. *Soft Matter* **2016**, *12* (9), 2542–2549. https://doi.org/10.1039/c5sm02693h.

(41) Dolmat, M.; Kozlovskaya, V.; Cropek, D.; Kharlampieva, E. Free-Standing Thin Hydrogels: Effects of Composition and PH-Dependent Hydration on Mechanical Properties. *ACS Appl. Polym. Mater.* **2021**, *3* (8), 3960–3971. https://doi.org/10.1021/acsapm.1c00511.

(42) Narayanan, R. P.; Melman, G.; Letourneau, N. J.; Mendelson, N. L.; Melman, A. Photodegradable Iron(III) Cross-Linked Alginate Gels. *Biomacromolecules* **2012**, *13*, 2465–2471.

(43) Yokoi, H.; Nomoto, E.; Ikoma, S. Reversible Formation of Iron(III) Ion Clusters in the Poly(Acrylic Acid)-Fe3+ Complex Gel with Changes in the Water Content. *J. Mater. Chem.* **1993**, *3* (4), 389–392. https://doi.org/10.1039/JM9930300389.

(44) Shuai, F.; Zhang, Y.; Yin, Y.; Zhao, H.; Han, X. Fabrication of an Injectable Iron (III) Crosslinked Alginate-Hyaluronic Acid Hydrogel with Shear-Thinning and Antimicrobial Activities. *Carbohydr. Polym.* **2021**, *260* (January), 117777. https://doi.org/10.1016/j.carbpol.2021.117777.

(45) Kang, M.; Oderinde, O.; Liu, S.; Huang, Q.; Ma, W.; Yao, F.; Fu, G. Characterization of Xanthan Gum-Based Hydrogel with Fe3+ Ions Coordination and Its Reversible Sol-Gel Conversion. *Carbohydr. Polym.* **2019**, *203* (July 2018), 139–147. https://doi.org/10.1016/j.carbpol.2018.09.044.

(46) Malhotra, A.; Bera, T.; Zhai, L. Bioinspired Metal Ion Coordinated Polyelectrolyte Fibrous Nanoreactors. *Adv. Mater. Interfaces* **2016**, *3* (22). https://doi.org/10.1002/admi.201600692.

(47) Dong, J.; Ozaki, Y.; Nakashima, K. FTIR Studies of Conformational Energies of Poly (Acrylic Acid) in Cast Films. *J. Polym. Sci. Part B Polym. Phys.* **1997**, *35* (3), 507–515. https://doi.org/10.1002/(SICI)1099-0488(199702)35:3<507::AID-POLB9>3.0.CO;2-O.

(48) Holten-Andersen, N.; Harrington, M. J.; Birkedal, H.; Lee, B. P.; Messersmith, P. B.; Lee, K. Y. C.; Waite, J. H. PH-Induced Metal-Ligand Cross-Links Inspired by Mussel Yield Self-Healing Polymer Networks with near-Covalent Elastic Moduli. *Proc. Natl. Acad. Sci. U. S. A.* **2011**, *108* (7), 2651–2655. https://doi.org/10.1073/pnas.1015862108.

(49) Peng, F.; Li, G.; Liu, X.; Wu, S.; Tong, Z. Redox-Responsive Gel-Sol/Sol-Gel Transition in Poly(Acrylic Acid) Aqueous Solution Containing Fe(III) Ions Switched by Light. *J. Am. Chem. Soc.* **2008**, *130* (48), 16166–16167. https://doi.org/10.1021/ja807087z.

(50) Chen, J.; Browne, W. R. Photochemistry of Iron Complexes. *Coord. Chem. Rev.* **2018**, *374*, 15–35. https://doi.org/10.1016/j.ccr.2018.06.008.

(51) Harvey, A. E.; Smart, J. A.; Amis, E. S. Simultaneous Spectrophotometric Determination of Iron(II) and Total Iron with 1,10-Phenanthroline. *Anal. Chem.* **1955**, *27* (1), 26–29. https://doi.org/10.1021/ac60097a009.

TOC Image